All-optical logic gates based on two-dimensional low-refractive-index nonlinear photonic crystal slabs

Ye Liu,[1,2] Fei Qin,[1] Zi-Ming Meng,[1] Fei Zhou,[1] Qing-He Mao,[2] and Zhi-Yuan Li[1,*]

[1]*Laboratory of optical physics, National Laboratory for condensed Mater Physics, Institute of Physics, Chinese Academy of Science, Beijing, 100190, China*

[2] *Anhui provincial key lab of photonics devices and materials, Anhui Institute of Optics and Fine Mechanics, Chinese Academy of Sciences, Hefei, 230031, China*

**lizy@aphy.iphy.ac.cn*

Abstract: This article demonstrates theoretical design of ultracompact all-optical AND, NAND, OR, and NOR gates with two-dimensional nonlinear photonic crystal slabs. Compound Ag-polymer film with a low refractive index and large third-order nonlinearity is adopted as our nonlinear material and photonic crystal cavities with a relatively high quality factor of about 2000 is designed on this polymer slab. Numerical simulations show that all-optical logic gates with low pump-power in the order of tens of MW/cm^2 can be achieved. These design results may provide very useful schemes and approaches for the realization of all-optical logic gates with low-cost, low-pump-power, high-contrast and ultrafast response-time.

OCIS codes: (230.5298) Photonic crystals; (230.1150) All-optical devices; (230.3750) Optical logic devices; (190.4390) Nonlinear optics, integrated optics.

References and links

1. Z. H. Li, and G. F. Li, "Ultrahigh-speed reconfigurable logic gates based on four-wave mixing in a semiconductor optical amplifier," IEEE Photon. Technol. Lett. **18**(12), 1341–1343 (2006).
2. Y. A. Zaghloul, and A. R. M. Zaghloul, "Complete all-optical processing polarization-based binary logic gates and optical processors," Opt. Express **14**(21), 9879–9895 (2006).
3. J. I. Cirac, and P. Zoller, "A scalable quantum computer with ions in an array of microtraps," Nature **404**(6778), 579–581 (2000).
4. Z. Zhao, A. N. Zhang, Y. A. Chen, H. Zhang, J. F. Du, T. Yang, and J. W. Pan, "Experimental demonstration of a nondestructive controlled-NOT quantum gate for two independent photon qubits," Phys. Rev. Lett. **94**(3), 030501 (2005).
5. J. Y. Kim, J. M. Kang, T. Y. Kim, and S. K. Han, "10 Gbit/s all-optical composite logic gates with XOR, NOR, OR and NAND functions using SOA-MZI structures," Electron. Lett. **42**(5), 303–304 (2006).
6. L. A. Wang, S. H. Chang, and Y. F. Lin, "Novel implementation method to realize all-optical logic gates," Opt. Eng. **37**(3), 1011–1018 (1998).
7. Z. J. Li, Z. W. Chen, and B. J. Li, "Optical pulse controlled all-optical logic gates in SiGe/Si multimode interference," Opt. Express **13**(3), 1033–1038 (2005).
8. T. K. Liang, L. R. Nunes, M. Tsuchiya, K. S. Abedin, T. Miyazaki, D. Van Thourhout, W. Bogaerts, P. Dumon, R. Baets, and H. K. Tsang, "High speed logic gate using two-photon absorption in silicon waveguides," Opt. Commun. **265**(1), 171–174 (2006).
9. V. M. N. Passaro, and F. De Leonardis, "All-optical AND gate based on Raman effect in silicon-on-insulator waveguide," Opt. Quantum Electron. **38**(9-11), 877–888 (2007).
10. T. Fujisawa, and M. Koshiba, "All-optical logic gates based on nonlinear slot-waveguide couplers," J. Opt. Soc. Am. B **23**(4), 684–691 (2006).
11. D. O. Guney, and D. A. Meyer, "Creation of entanglement and implementation of quantum logic gate operations using a three-dimensional photonic crystal single-mode cavity," J. Opt. Soc. Am. B **24**(2), 283–294 (2007).
12. D. V. Novitsky, "Effect of frequency detuning on pulse propagation in one-dimensional photonic crystal with a dense resonant medium: application to optical logic," J. Opt. Soc. Am. B **26**(10), 1918–1923 (2009).
13. D. V. Novitsky, and S. Y. Mikhnevich, "Logic Gate Based on a One-Dimensional Photonic Crystal Containing Quantum Dots," J. Appl. Spectrosc. **77**(2), 232–237 (2010).
14. I. V. Dzedolik, S. N. Lapayeva, and A. F. Rubass, "All-optical logic gates based on nonlinear dielectric films," Ukr. J. Phys. Opt. **9**(3), 187–196 (2008).
15. I. S. Nefedov, V. N. Gusyatnikov, P. K. Kashkarov, and A. M. Zheltikov, "Low-threshold photonic band-gap optical logic gates," Laser Phys. **10**(2), 640–643 (2000).

#138864 - $15.00 USD Received 30 Nov 2010; revised 28 Dec 2010; accepted 6 Jan 2011; published 18 Jan 2011

16. Y. L. Zhang, Y. Zhang, and B. J. Li, "Optical switches and logic gates based on self-collimated beams in two-dimensional photonic crystals," Opt. Express **15**(15), 9287–9292 (2007).
17. P. Andalib, and N. Granpayeh, "All-optical ultracompact photonic crystal AND gate based on nonlinear ring resonators," J. Opt. Soc. Am. B **26**(1), 10–16 (2009).
18. P. Andalib, and N. Granpayeh, "All-optical ultra-compact photonic crystal NOR gate based on nonlinear ring resonators," J. Opt. A, Pure Appl. Opt. **11**(8), 085203 (2009).
19. J. B. Bai, J. Q. Wang, J. Z. Jiang, X. Y. Chen, H. Li, Y. S. Qiu, and Z. X. Qiang, "Photonic NOT and NOR gates based on a single compact photonic crystal ring resonator," Appl. Opt. **48**(36), 6923–6927 (2009).
20. A. de Rossi, M. Lauritano, S. Combrie, Q. V. Tran, and C. Husko, "Interplay of plasma-induced and fast thermal nonlinearities in a GaAs-based photonic crystal nanocavity," Phys. Rev. A **79**(4), 043818 (2009).
21. A. Baron, A. Ryasnyanskiy, N. Dubreuil, P. Delaye, Q. Vy Tran, S. Combrié, A. de Rossi, R. Frey, and G. Roosen, "Light localization induced enhancement of third order nonlinearities in a GaAs photonic crystal waveguide," Opt. Express **17**(2), 552–557 (2009).
22. M. Notomi, A. Shinya, S. Mitsugi, G. Kira, E. Kuramochi, and T. Tanabe, "Optical bistable switching action of Si high-Q photonic-crystal nanocavities," Opt. Express **13**(7), 2678–2687 (2005).
23. V. R. Almeida, C. A. Barrios, R. R. Panepucci, and M. Lipson, "All-optical control of light on a silicon chip," Nature **431**(7012), 1081–1084 (2004).
24. F. Raineri, C. Cojocaru, P. Monnier, A. Levenson, R. Raj, C. Seassal, X. Letartre, and P. Viktorovitch, "Ultrafast dynamics of the third-order nonlinear response in a two-dimensional InP-based photonic crystal," Appl. Phys. Lett. **85**(11), 1880–1882 (2004).
25. M. W. McCutcheon, G. W. Rieger, J. F. Young, D. Dalacu, P. J. Poole, and R. L. Williams, "All-optical conditional logic with a nonlinear photonic crystal nanocavity," Appl. Phys. Lett. **95**(22), 221102 (2009).
26. Y. Wang, X. B. Xie, and T. Goodson 3rd, "Enhanced third-order nonlinear optical properties in dendrimer-metal nanocomposites," Nano Lett. **5**(12), 2379–2384 (2005).
27. X. Y. Hu, P. Jiang, C. Xin, H. Yang, and Q. H. Gong, "Nano-Ag:polymeric composite material for ultrafast photonic crystal all-optical switching," Appl. Phys. Lett. **94**(3), 031103 (2009).
28. X. Y. Hu, P. Jiang, C. Y. Ding, H. Yang, and Q. H. Gong, "Picosecond and low-power all-optical switching based on an organic photonic-bandgap microcavity," Nat. Photonics **2**(3), 185–189 (2008).
29. X. Y. Hu, Y. H. Liu, J. Tian, B. Y. Cheng, and D. Z. Zhang, "Ultrafast all-optical switching in two-dimensional organic photonic crystal," Appl. Phys. Lett. **86**(12), 121102 (2005).
30. Y. H. Liu, X. Y. Hu, D. X. Zhang, B. Y. Cheng, D. Z. Zhang, and Q. B. Meng, "Subpicosecond optical switching in polystyrene opal," Appl. Phys. Lett. **86**(15), 151102 (2005).
31. Y. Liu, F. Qin, Z. Y. Wei, Q. B. Meng, D. Z. Zhang, and Z. Y. Li, "10 fs ultrafast all-optical switching in polystyrene nonlinear photonic crystals," Appl. Phys. Lett. **95**(13), 131116 (2009).
32. Y. Liu, F. Qin, F. Zhou, and Z. Y. Li, "Ultrafast and low-power photonic crystal all-optical switching with resonant cavities," J. Appl. Phys. **106**(8), 083102 (2009).
33. K. M. Ho, C. T. Chan, and C. M. Soukoulis, "Existence of a photonic gap in periodic dielectric structures," Phys. Rev. Lett. **65**(25), 3152–3155 (1990).
34. R. D. Meade, K. D. Brommer, A. M. Rappe, and J. D. Joannopoulos, "Existence of a Photonic Band-Gap in 2 Dimensions," Appl. Phys. Lett. **61**(4), 495–497 (1992).
35. S. Datta, C. T. Chan, K. M. Ho, and C. M. Soukoulis, "Photonic band gaps in periodic dielectric structures: The scalar-wave approximation," Phys. Rev. B Condens. Matter **46**(17), 10650–10656 (1992).
36. A. F. Oskooi, D. Roundy, M. Ibanescu, P. Bermel, J. D. Joannopoulos, and S. G. Johnson, "MEEP: A flexible free-software package for electromagnetic simulations by the FDTD method," Comput. Phys. Commun. **181**(3), 687–702 (2010).
37. Y. Akahane, T. Asano, B. S. Song, and S. Noda, "High-Q photonic nanocavity in a two-dimensional photonic crystal," Nature **425**(6961), 944–947 (2003).

1. Introduction

In recent years, all-optical logic gates, which can fulfill various logical function operations, have received much attention for their potential applications in ultrafast information processing [1,2], all-optical computing systems [3,4], and so on. There are several methods to realize all-optical logic functions, such as semiconductor optical amplifier (SOA) [5], optical interference effect [6,7], and third-order nonlinear effect [8–10]. Nowadays, all-optical logic gates based on the third-order nonlinear effect of photonic crystal (PhC) structures have received increasing attention. Various PhC structures have been designed and discussed [11–15]. For example, Zhang et. al. proposed optical logic OR and XOR gates based on the interference of reflected and transmitted self-collimated beams in a two-dimensional (2D) PhC waveguide [16]. Anadalib et. al. proposed ultra-compact photonic crystal "AND" gate [17] and "NOR" gate [18] theoretically based on PhC nonlinear ring resonators. Bai et. al. demonstrated photonic NOT and NOR gates based on a single compact PhC ring resonator [19].

#138864 - $15.00 USD Received 30 Nov 2010; revised 28 Dec 2010; accepted 6 Jan 2011; published 18 Jan 2011

However, we notice that most works of PhC all-optical logic gates focus on 2D PhC structures, where the thickness of PhCs is regarded as infinite. When considering their practical applications, ultracompact all-optical logic gates realized in 2D PhC slabs are more prospective. Such 2D PhC slabs provide confinement of light in the vertical direction by total internal reflection and allow control of light with the PhC in the plane of the slab. This type of PhCs is much simpler for fabrication than three-dimensional (3D) PhCs and has great potentiality as ultracompact integrated optical devices. So, in this article, we focus on the design of all-optical logic gates in the platform of 2D PhC slabs.

As is known, the characteristics of all-optical PhC logic gates mainly depend on the properties of the selected nonlinear material. Two kinds of nonlinear materials are widely used. One is the semiconductor materials, such as GaAs [20,21], Si [22,23], and InP [24,25]. The nonlinearity originates from the two-photon absorption (TPA) effect of free carrier in semiconductors. These semiconductor materials possess a relatively high refractive index (higher than 2.0), which can provide complete photonic band gaps and good confinement of photons in the cavities. However, the third-order nonlinear optical susceptibility of these semiconductor inorganic materials is relatively low (in the order of 10^{-12} esu) and their nonlinear response time is relatively long (in the order of nanoseconds), which restrict their practical applications on low pump power and ultrafast response time all-optical devices. Another popular nonlinear material is the π-conjugation organic polymer materials, which have more prominent nonlinear optical properties, such as large third-order nonlinear optical susceptibility (in the order of 10^{-9} esu) and ultrafast nonlinear response time (in the order of femtoseconds). Furthermore, recent studies show that a larger third-order nonlinear susceptibility (in the order of 10^{-6} to 10^{-7} esu) can be easily obtained by adding some metal nanoparticles [26,27] or dye molecules [28] into the organic films, and this allows one to reduce the pump power of all-optical devices efficiently. At the same time, these organic materials may possess ultrafast nonlinear response time in the order of several picoseconds [29] or even femtoseconds [30–32]. In this article, we adopt compound Ag-polymer film as our nonlinear material, whose linear refractive index is 1.59 and third-order nonlinear susceptibility is set at 1.0×10^{-7} esu. The polymer is polystyrene, which has a large third-order nonlinearity and ultrafast nonlinear optical response speed down to several femtoseconds [30–32].

This article is arranged as follows. In Sec. 2 we first design PhC cavities with a relatively high quality factor on 2D low-index Ag-polymer PhC slabs. Different PhC cavities are analyzed and discussed. PhC cavities with a modest quality factor around 2000 are adopted for the design of all-optical logic gates on consideration of the precision and repeatability in the fabrication of these structures. The nonlinear optical properties of these PhC cavities are investigated. In Sec. 3 we discuss the principles of various all-optical logic gates based on PhC structures with double cavities. The detailed scheme of the design results of all-optical AND, NAND, OR, and NOR gates with PhC cavities on the 2D Ag-polymer slab are presented and discussed. In Sec. 4 we conclude this article.

2. Design and nonlinear properties of 2D PhC slab cavities in Ag-polymer films

For realizing low pump power and ultrafast response time all-optical logic gates, PhC cavities with a relatively high quality factor are necessary. Our PhC structure is formed by etching periodical air holes on the Ag-polymer film, and the cavities are obtained by removing some air-holes at suitable positions, see Fig. 1(a). The linear refractive index of the film is 1.59. Because of the low refractive index contrast between the film and air, it is not a good candidate for the design of PhC structures with a complete band gap [33–35], and the cavity here is mainly based on the directional photonic band gap confinement of light. That is to say, in our structure, an eigenmode with the frequency in the band gap along the $\Gamma - X$ direction may become leaky along the $\Gamma - M$ direction, which makes the point defect not suitable for the design of high quality factor (high-Q) cavities. Based on this consideration, we adopt the

#138864 - $15.00 USD Received 30 Nov 2010; revised 28 Dec 2010; accepted 6 Jan 2011; published 18 Jan 2011

"line defect" cavity, which is formed by removing several air holes along the longitudinal direction (y-axis) in the middle of this structure.

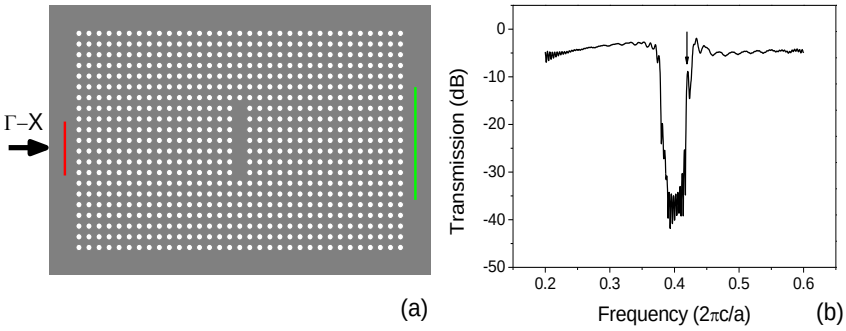

Fig. 1. (a) The PhC "line defect" cavity on a 2D PhC slab; (b) The corresponding band gap along $\Gamma - X$ direction.

Let us consider the PhC structure as shown in Fig. 1(a). The air-bridge 2D PhC film formed by etching periodical square lattice of air holes is adopted. The radius of the air holes is $0.25a$, where a is the lattice constant. The thickness of this slab is $1.5a$. The "line defect" is formed by removing the center seven air holes along the y-axis. In this article, MEEP which is a free finite-difference time-domain software package developed by MIT photonic crystal group is adopted as our simulation tool [36]. Firstly, we calculate the transmission spectrum along the $\Gamma - X$ direction by the 3D finite-difference time-domain (FDTD) method, and the result is shown in Fig. 1(b). In the simulation, an area light source located at the left end of the PhC structure [marked with red line in Fig. 1(a)] is used, and the incident light is propagating along the $\Gamma - X$ direction. At the right end of the PhC structure, a receiver plane [marked with green line in Fig. 1(a)] is adopted to record the transmission power and measure the transmission spectrum. Both the lengths along y- and z- axes of the receiver plane are twice as long as those of the source plane. And the receiver area is 4 times as large as the source area so that all the transmission powers, including those that are scattered and diverge away from the $\Gamma - X$ direction are collected. From this result, we can find a defect mode appears near the high-frequency band gap edge (marked with the black arrow in Fig. 1(b)). This mode will interact with the band edge mode, and the interaction results in a very low quality factor of about 20.

In order to improve the quality factor of this cavity, we make some optimization of this structure following the scheme as shown in Fig. 2(a). The optimization approach is almost the same with the high-Q cavity design on Si-based PhC slabs [37]. Only the geometry parameters of the air holes nearby the cavity are changed. The air holes of the nearest neighboring two rows (labeled with "a" holes) are shifted away with $0.2a$, and the air holes of the second nearest neighboring two rows (labeled with "b" holes) are shifted away with $0.1a$. At the same time, the radius of these four rows of air holes is changed from $0.25a$ to $0.2a$. We calculate the transmission spectrum of this structure, and the result is shown in Fig. 2(c). By fine tuning the geometry parameters of the PhC cavity in the above manner, the defect mode has been shifted to the middle of band gap, which can improve the quality factor of the cavity. The electric field distribution of this optimized PhC cavity with the incidence of resonance frequency is shown in Fig. 2(b). Here, the normalized electric field amplitude ($|\mathbf{E}|$) is considered. We can find that due to the low-refractive-index of the substrate, the mode volume of this cavity mode is relatively large, whose length is about $14a$ along the x-axis. So, in the following design of all-optical logic gates, if the distance between the input / output waveguides and the cavity is longer than $15a$, the introduction of the waveguide will not influence the mode profile of the cavity mode. Figure 2(d) shows the frequency spectrum of this cavity mode, from which we can find that the quality factor reaches 1558. Here the

#138864 - $15.00 USD Received 30 Nov 2010; revised 28 Dec 2010; accepted 6 Jan 2011; published 18 Jan 2011

transmission spectrum has been normalized with respect to its peak value. Although this quality factor is not very large, considering the experimental precision and repeatability in the sample fabrication, such a cavity is suitable for the practical experiment analysis. Therefore, in the following we will adopt the cavity with a quality factor around 2000 for the design of all-optical logic gates.

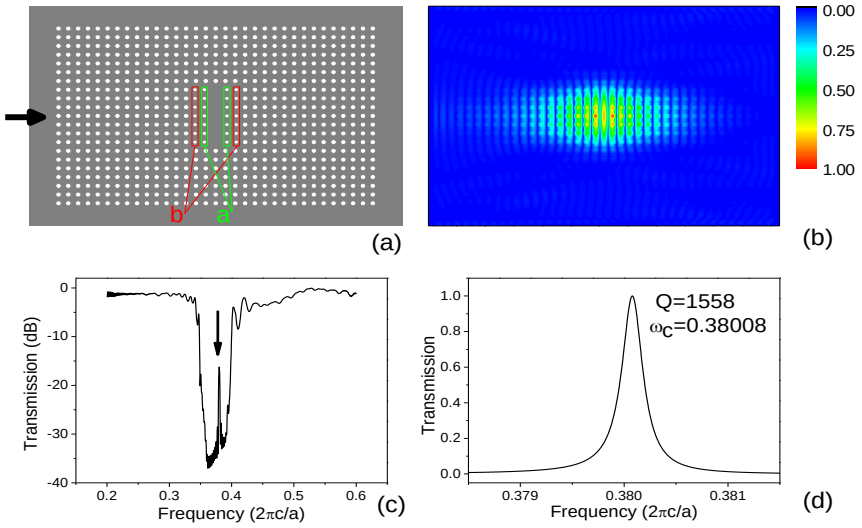

Fig. 2. (a) The schematic structure of optimized PhC cavity. (b) The electric field distribution at the resonant frequency of the optimized PhC cavity. (c)The calculated transmission spectrum. (d) The optimized cavity mode. The normalized resonant frequency is 0.38008, and the quality factor is 1558.

Furthermore, we find that the properties of the PhC cavities are associated with their lengths along the y-axis. Here, we show the change of the normalized frequency and quality factor for different cavities in Table 1. The "Lm" cavity corresponds to a cavity whose length along the y-axis is *m* times the lattice constant. From these results, we find that the normalized frequency of cavity shifts to lower frequency and the quality factor gets larger with the increase of the cavity length along the y-axis. This result will be very useful for the design of multiple cavities to realize all-optical logic gates with various functions.

Table 1. The influence on the frequency and quality factor with different lengths along the y-axis of cavities.

Cavity type	Normalized frequency	Quality factor
L3	0.38451	638
L5	0.38135	1287
L6	0.38060	1367
L7	0.38008	1558
L8	0.37971	1765
L9	0.37943	1936

Next, we discuss the nonlinear properties of this cavity mode under the excitation of external pump light. With the incident pump light, the refractive index of the Ag-polymer film will be changed. In our case, the third-order nonlinear susceptibility of Ag-polymer film is set at 1.0×10^{-7} esu , so with the pump light, the refractive index will increase and the defect mode will shift to lower frequency. Figure 3 shows the shift of the defect mode of a L7-type cavity with and without the pump light. When the pump power is 45 MW/cm^2, the normalized resonant frequency of the defect mode shifts from 0.38008 to 0.37932 ($2\pi c/a$), where c is the speed of light in vacuum and a is the lattice constant of the PhC. Here the transmission spectrum has also been normalized with respect to its peak value. If the lattice constant is

#138864 - $15.00 USD Received 30 Nov 2010; revised 28 Dec 2010; accepted 6 Jan 2011; published 18 Jan 2011

$a = 590$ nm, the corresponding wavelength shifts from 1552.3 nm to 1555.4 nm. Due to the relatively high quality factor of this cavity (Q = 1558), the spectrum width of the defect mode is very narrow (about 1 nm), which make high transmission contrast with and without pump light.

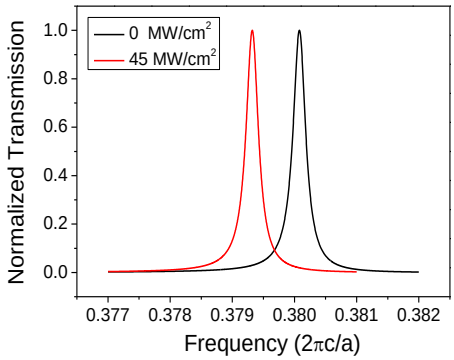

Fig. 3. The shift of defect mode under pump light. The black line corresponds to the linear case, and the red line represents the nonlinear case with the pump power of 45 MW/cm^2. The transmission is normalized to its peak value.

3. Principle and realization of all-optical logic gates

Until now, we have designed relatively high-Q PhC cavities on the low refractive index Ag-polymer film, and discussed the nonlinear optical properties of these PhC cavities. In the following, we show the principle of all-optical logic gates and demonstrate the design results for various all-optical logic gates.

The 2D PhC slab we studied for all-optical logic gates is shown in Fig. 4. For realizing various logic functions, this structure contains two cavities. The input signal light is divided into two paths by an input Y-type waveguide, and then interacts with the two cavities. At last, they are coupled to an output Y-type waveguide together. At the same time, two pump lights I_1 and I_2 are incident onto the upper surface of the PhC structure normally. Considering the experimental conditions that the area of PhC structures is less than 400 μm^2 and the focus radius of pump light is about 10 μm, both of the pump lights will interact with the two cavities. In our designs here, the input signal is a continuous wave with the power of 0.5 kW/cm^2, while the pump lights are picosecond ultrashort pulses whose average pulse powers are in the order of 10 MW/cm^2. The following designs of all-optical logic gates are all based on this consideration. Notice that polystyrene has an optical response time on the order of several femtoseconds, which is much faster than the pump pulse duration time (on the order of picoseconds) [30–32]. Furthermore, the cavity quality factor is only modest (about 2000), so that the lifetime of the cavity is also on the order of picoseconds. This means that the switching rate of each nonlinear cavity and the logic gates should be mainly determined by the duration of the picosecond pump pulses. Therefore, the switching rate should also be on the order of picoseconds.

#138864 - $15.00 USD Received 30 Nov 2010; revised 28 Dec 2010; accepted 6 Jan 2011; published 18 Jan 2011

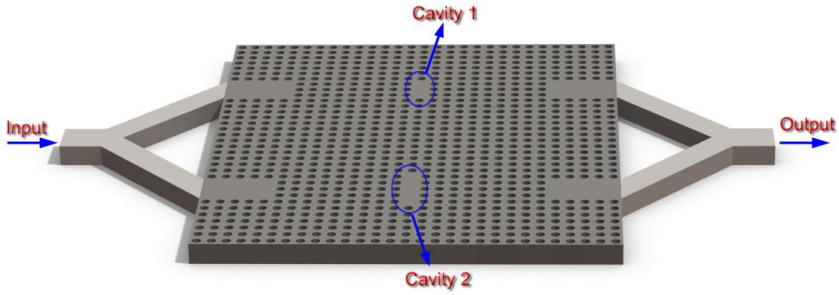

Fig. 4. Schematic structure of 2D PhC slab for all-optical logic gates.

By suitable selection of the resonant frequencies of these two cavities, we can realize all-optical logic gates with different logic functions. Here, at each path, the distance between the input or output waveguide and the cavity is $16a$, and the existence of waveguides will not influence the properties of the cavity mode. The frequency of the input probe light is denoted as f_0, while the resonant frequencies of the two cavities are f_1 and f_2, respectively. Table 2 shows the principles of all-optical AND, NAND, OR, and NOR gates, respectively.

Table 2. The principles of all-optical AND, NAND, OR, and NOR gates

Logic gate	Initialization	I_1	I_2	I_1 & I_2
AND ($f_1 = f_2$)	$f_1 \neq f_0$ logic 0	$f_1 \neq f_0$ logic 0	$f_1 \neq f_0$ logic 0	$f_1 = f_0$ logic 1
NAND ($f_1 \neq f_2$)	$f_2 = f_0$ logic 1	$f_1 = f_0$ logic 1	$f_1 = f_0$ logic 1	$f_1 \neq f_0, f_2 \neq f_0$ logic 0
OR ($f_1 \neq f_2$)	$f_1 \neq f_0, f_2 \neq f_0$ logic 0	$f_2 = f_0$ logic 1	$f_2 = f_0$ logic 1	$f_1 = f_0$ logic 1
NOR ($f_1 = f_2$)	$f_1 = f_0$ logic 1	$f_1 \neq f_0$ logic 0	$f_1 \neq f_0$ logic 0	$f_1 \neq f_0$ logic 0

For the AND gate, both of the two cavities are selected as the L7-type cavity, whose quality factor is about 1558, and the normalized resonant frequency is $f_1 = f_2 = 0.38008$. The normalized frequency of the input signal light is set at $f_0 = 0.37932$. At first, due to the frequency deflection between the input signal light and the cavity mode, the signal light is localized at the forbidden gap, and its transmission is as low as 1.9%. With the incidence of single pump light I_1 or I_2, the refractive index of Ag-polymer increases, and the resonant frequency of cavity will shift to lower frequency. When the pump power is 22.5 MW/cm^2, which makes the refractive index change by 0.2%, the nonlinear resonant frequency shifts to 0.3797. In this case, although the frequency deflection between the input signal light and the cavity mode become less, due to the narrow spectrum width, the transmission is still low, which is about 9.5%. Under the excitation of both pump lights I_1 and I_2, the frequency of defect mode shifts to the frequency of the input signal light exactly, and the transmission reaches to 100%. Table 3 shows the truth table of the AND gate. Here, we should notice that in our design of all-optical logic gates, the transmission in each case is monitored at the output waveguide and calculated by Pade approximate method. And the transmission here is normalized to its peak value, not to the input signal light.

Table 3. Truth table of the AND gate

pump1		pump2		Output	
Power (MW/cm^2)	Logic level	Power (MW/cm^2)	Logic level	Transmission (%)	Logic level
0	0	0	0	1.9	0
22.5	1	0	0	9.5	0
0	0	22.5	1	9.5	0
22.5	1	22.5	1	100	1

#138864 - $15.00 USD Received 30 Nov 2010; revised 28 Dec 2010; accepted 6 Jan 2011; published 18 Jan 2011

Let us turn to the NAND gate. Here, the two cavities are L7-type (f_1 = 0.38008, Q = 1558) and L8-type (f_2 = 0.37971, Q = 1765), respectively. The normalized frequency of the signal light is set at f_0 = 0.37971, which is just the same with the resonant frequency of cavity 2. Without the pump lights, the input signal light will be coupled with cavity 2, and the transmission is nearly 100%. With single pump light I_1 or I_2, the resonant cavity mode will shift to lower frequency. As a result, the resonant frequency of cavity 2 will deflect away from the frequency of the signal light, but the resonant frequency of cavity 1 will be nearer to the frequency of the signal light. When the pump power is 22 MW/cm^2, the signal light will be coupled with cavity 1, and the transmission can also be 100%. If both of the pump lights I_1 and I_2 interact with the PhC structure, the resonant frequency of cavities will deflect the frequency of the signal light again, which makes the transmission decrease remarkably. The truth table of the NAND gate is shown in Table 4.

Table 4. Truth table of NAND gate

pump1		pump2		Output	
Power (MW/cm^2)	Logic level	Power (MW/cm^2)	Logic level	Transmission (%)	Logic level
0	0	0	0	100	1
22	1	0	0	100	1
0	0	22	1	100	1
22	1	22	1	7.1	0

Table 5. Truth table of the OR gate

pump1		pump2		Output	
Power (MW/cm^2)	Logic level	Power (MW/cm^2)	Logic level	Transmission (%)	Logic level
0	0	0	0	1.9	0
42.5	1	0	0	90.1	1
0	0	42.5	1	90.1	1
42.5	1	42.5	1	100	1

Next, the OR gate is designed with the structure shown in Fig. 4. Two kinds of cavities with L6-type (f_1 = 0.3806, Q = 1367) and L7-type (f_2 = 0.38008, Q = 1558) are adopted. The frequency of the signal light is f_0 = 0.37932, which is not resonant with any cavity. So, at first, the transmission of signal light is very low, only 1.9%, corresponding to the logic "0" of the OR gate. Under the excitation of single pump light whose power is 42.5 MW/cm^2, the frequency of cavity 2 (f_2) will shift to the frequency of the signal light (f_0 = 0.37932), and the transmission is 90.1%. With the incidence of two pump lights, the resonant frequency of cavity 1 (f_1) shifts to f_0, and the transmission from the output reaches 100%. The truth table of the OR gate is shown in Table 5.

Table 6. Truth table of the NOR gate

pump1		pump2		Output	
Power (MW/cm^2)	Logic level	Power (MW/cm^2)	Logic level	Transmission (%)	Logic level
0	0	0	0	100	1
22.5	1	0	0	8.1	0
0	0	22.5	1	8.1	0
22.5	1	22.5	1	1.9	0

Finally, we show the design results of the NOR gate. In this case, both of the two cavities are selected as the L7-type cavity (f_1 = f_2 = 0.38008, Q = 1558). The frequency of the input signal light is set at f_0 = 0.38008, which is the same with the resonant frequency of the cavities. The transmission is as high as 100% without pump lights. Under the pump light, the resonant frequency of cavity will shift to lower frequency, and far away from the frequency of the signal light. When the pump power is 22.5 MW/cm^2, the resonant frequency of the cavities shifts to 0.3797, and the transmission is 8.1% with single pump light excitation. The

#138864 - $15.00 USD Received 30 Nov 2010; revised 28 Dec 2010; accepted 6 Jan 2011; published 18 Jan 2011

transmission will be lower with the interaction of two pump lights. Table 6 shows the truth table of the NOR gate.

4. Conclusion

In summary, we have presented design of all-optical logic gates with different functions by means of PhC cavities that are built in the platform of low refractive index nonlinear Ag-polymer films. We have accomplished design of relatively high-Q cavities whose quality factor is around 2000 on the 2D low refractive index square-lattice PhC slab. We find that the resonant frequency of the "line defect" cavities can be adjusted with the cavity length, which makes possible the design of various all-optical logic gates.

By combining two "line defect" cavities and imposing appropriate conditions on the resonant frequency of cavities and the pump power, we have demonstrated all-optical AND, NAND, OR, and NOR gates in 2D Ag-polymer PhC slabs. The pump power as low as tens of MW/cm^2 has been sufficiently large to pump the logic gates. More logic function devices can be designed by our PhC structures. Because of the prominent nonlinear optical properties (large third-order optical nonlinear susceptibility and ultrafast nonlinear response time) and low-cost of compound Ag-polymer films, this work may be useful for designing and realizing devices that can find practical applications in all-optical integration, all-optical information processing and optical computing.

Acknowledgement

This work is supported by the National Natural Science Foundation of China under Grant No. 10634080 and the National Basic Research Foundation of China under Grant Nos. 2007CB936603 and 2007CB935703.

#138864 - $15.00 USD Received 30 Nov 2010; revised 28 Dec 2010; accepted 6 Jan 2011; published 18 Jan 2011